

ON MICROSTRUCTURE DEVELOPMENT AND INCLUSION GENERATION IN A CONTINUOUSLY CAST RESULPHURISED STEEL

C. MAPELLI[†], M. VEDANI[†] AND A. ZAMBON[‡]

[†] Politecnico di Milano - Dipartimento di Meccanica, Piazza L. Da Vinci 32, I-20133 Milano, Italy
carlo.mapelli@polimi.it, maurizio.vedani@polimi.it

[‡] Università di Padova - DIMEG, Via Marzolo 9, I-35131 Padova, Italy
zambona@ux1.unipd.it

Abstract— An experimental study on solidification structure development and on endogenous inclusion precipitation in a continuously cast resulphurised steel is presented. Results were obtained by investigating two heats of a free cutting C-Mn steel cast in billets with a diameter of 145 mm. The as cast structure was evaluated by macro- and microscopic analyses. Primary and secondary dendrite arm spacing measurement allowed to estimate the solidification time experienced by the steel in different region of the billet section. Modification of the pearlite vs. ferrite fraction was also studied as a function of distance from billet surface and thus with reference to solidification conditions. Endogenous inclusions of the type MnS and CaO-Al₂O₃ were analysed. Their formation was discussed as a function of the composition of the heats. Also for the inclusions resulting after steel solidification, the data suggested that the effects of local solidification condition and of segregation played a role of primary importance.

Keywords— continuous casting, resulphurised steels, dendrite arm spacing, endogenous inclusions.

I. INTRODUCTION

Over recent decades continuous casting has become a vital part of the steelmaking process due to improved yield and lower energy consumption properties. Concurrently the classical ingot route underwent a dramatic loss of interest and remains competitive only in specialized areas. Steel slabs and billets produced by continuous casting possess a significantly different structure from the products of ingot technology. A full knowledge of the factors affecting structure (e.g. columnar vs. equiaxed structure), segregation of alloying elements, defects formation and inclusion generation is of paramount importance for any further improvement required to increase productivity and quality of continuous casting plants.

A first aspect of great concern in steel products is the billet structure in terms of equiaxed vs. columnar grains. Several investigations were published on the

effects of carbon content, on liquid superheat, on peritectic transformation and on solidification parameters [Irving *et al.*, 1984]. In general terms, the tendency toward columnar or equiaxed structure depends primarily on steel composition. Compositions with intermediate C contents (from 0,10 to 0,50% C) tend to crystallise with an equiaxed central structure [Jacobi and Wünnenberg, 1997]. A large proportion of equiaxed structure is generally recognized as beneficial due to improved segregation distribution and cracking resistance. To this aim, great research effort was devoted to stirring effects and soft reduction (either of thermal or mechanical type) in plant design [Jacobi and Wünnenberg, 1997; Sivesson *et al.* 1998; El-Bealy and Fredriksson, 1994].

Internal quality, mainly evaluated by crack formation and centreline or intercolumnar segregations is a factor substantially governed by strand geometry and by solidification conditions. Again, a fully columnar structure is not appreciated since it increases segregation on the centreline. Amongst the factors affecting segregation is product bulging in the final stages of solidification. When ferrostatic pressure reaches high levels and the constraint imparted by the strand rolls is not adequate, billet or slab thickness can increase. Solute enriched liquid can thus flow through the centreline and solidify as central segregation even if the original structure is of equiaxed type. Similar effects are also reported to be brought about by internal solidification shrinkage that promote a flow of carbon-enriched steel in the final solidification region in the centre of the cast material [Irving *et al.*, 1984; Jacobi and Wünnenberg, 1997; Sivesson *et al.* 1998; El-Bealy and Fredriksson, 1994]. To counteract this phenomenon, a gradual tapering of the roll gaps in the zone of final solidification revealed to be an effective method. A further beneficial effect of this technology is the squeezing action of the strand that may crush the tips of the dendrites of the advancing columnar grains.

Microsegregation behaviour in continuously cast steels is a concurrent aspect that roughly depends on the same variables discussed above. Evaluation of microsegregation is often performed in terms of dendrite arm spacing (DAS) which is considered as a measure of the segregation distance of crystal development during

solidification. From a experimental point of view, reference is usually made to the secondary dendrite arm spacing (SDAS) as evaluated by optical microscopy techniques. In published literature SDAS was correlated for many steel grades to solidification and cooling conditions – the related variables can be the cooling rate (CR), the temperature gradient at liquidus line (G), the solid front growth rate (R) – as well as to chemical composition and secondary cooling conditions. The growth law can be described as a function of CR by a equation of the type: $SDAS = c_1 \cdot CR^k$, being c_1 and k material and system constants. For practical purposes or when the heat flux conditions on solidification are not directly measured, reference is often made to SDAS as a function of the distance from product surface (chill surface). Again the data can be readily fitted by equations of the form: $SDAS = c_2 \cdot x^n$, being c_2 and n materials and system constants and x the distance from surface [Weisgerber *et al.*, 1999; Senk *et al.*, 1999].

Manganese is a widely used alloying element in carbon steels. Its segregation tendency is also well known and of great practical interest. Senk and co-authors published a set of experimental data collected by investigating unalloyed carbon steels with carbon content ranging from 0,2 to 0,7% and produced with thicknesses from 60 mm down to 1,9 mm (from ingot casting simulating the thin slab casting process to twin roll casting were considered for this purpose) [Senk *et al.*, 1999]. It was shown that the segregation coefficient for manganese (c_{max}/c_{min} ratio) increased from surface to centre of cast products and was also directly related to carbon content and to cooling rate.

During recent years a relatively huge research activity was also dedicated to thermochemistry and precipitation kinetics of inclusions in steels and to the interaction of the inclusions with the solidification front. To efficiently control the reactions taking place during steel refining and solidification, predictive models based on thermodynamical approaches were developed [Eriksson and Hack, 1990; Lu *et al.*, 1994; Cicuti *et al.*, 1997; Dyson *et al.*, 1998; Hassall *et al.*, 1998; Lehmann *et al.*, 1998; Hong *et al.*, 1995; Presern *et al.*, 1991; Mapelli *et al.*, 2000]. Models revealed to be an efficient tool for the evaluation of the equilibria between slag and metal and for the assessment of the precipitation of endogenous inclusions (complex oxides, sulphides, nitrides) within the liquid steel as a function of temperature and elemental activities.

The interaction of inclusions with the solidifying steel has been the subject of several papers that approached different aspects of this phenomenon. On a macroscale, the flow behaviour of the steel in the mould was modelled and the transport phenomena of the inclusions were computed in a research developed by Grimm and co-authors [Grimm *et al.*, 1999]. Removal rate by flotation at the meniscus and entrapment in the solidified steel could thus be evaluated. It is of particular significance the ability of the model to reproduce, at least in a semiquantitative manner, the development of inclu-

sion concentration at a specific distance from slab loose side (often known as quarterline band or quarter inclusion pile-up) and the formation of multiple inclusion bands as a consequence of irregular steel flow in the mould.

The present paper is aimed at widening the existing data and observations about solidification and inclusion formation in a resulphurised steel grade produced by continuous casting. Especially, experimental data on structure and endogenous inclusions properties were gathered and discussed in terms of product homogeneity and of inclusion distribution as a function of billet position (extrados vs. intrados).

I. MATERIALS AND EXPERIMENTAL PROCEDURES

The material investigated in the present study was a resulphurised C-Mn Al-killed steel. It is produced by scrap melting in a 98 ton E.B.T. electric arc furnace. Secondary steelmaking is carried out in a 90 ton ladle furnace. In particular, after the initial deoxidation, the standard ladle furnace treatment consists of desulphurisation with CaO and CaFe alloy and concurrent argon bubbling through nozzles positioned at the ladle bottom. Following overheating and temperature setting, the steel is resulphurised by FeS wire addition and subsequently Ca treated by CaSi injection. After refining, the steel is continuously cast in a curved four-strand machine to produce billets having a diameter of 145 mm.

Two different heats of the resulphurised steel were investigated in this study with the aim of gathering further information on repeatability of structural and inclusion distribution features. Their chemical composition is given in Table 1.

Heat	C	Mn	S	Al	Ca	N
B1	0.8	1.43	0.028	0.023	0.0012	0.0090
B2	0.19	1.46	0.028	0.025	0.0011	0.0081

Table 1. Composition of the C-Mn resulphurised steel heats investigated in the present study (mass %)

Sections of the continuously cast billets were cut transversally and longitudinally with respect to billet axis. Macrographs of the solidification structures were obtained by sulphur printing technique. Metallographic samples were then cut from the sections of the billets at specific locations and prepared for microstructural observation by grinding and polishing. After optical microscope analyses for detection of inclusion distribution, the samples were observed in a scanning electron microscope (SEM) equipped with a X-ray energy dispersive spectrometer (EDS) system. Inclusions were analysed quantitatively for their identification.

The measure of the volume fraction and of the shape of the non-metallic inclusions was performed by analysing selected areas on the section of the billets. The total number of the areas observed was 117 having a size of

0,34mm² each. Measurements were carried out on six different directions equally spaced and crossing the geometrical centre of the billet.

Data on the chemical composition and temperature of the steel during casting were also collected. These were then used as input for a thermodynamic model aimed at predicting the type and amount of inclusions formed in the steel. Details of the model structure were published elsewhere [Mapelli *et al.*, 2000]. The model is based on the Fe-Al-Ca-O-S equilibrium system and allows to solve the equilibrium reactions for the formation of oxides and sulphides through an iterative procedure coupled by mass balance equations. The results of the calculation were used here as a basis for discussion on the experimental results obtained.

III. RESULTS AND DISCUSSION

A. Macrostructure

The sulphur prints obtained for the transverse and longitudinal sections of the billets B1 and B2 showed a ring close to the surface, whose thickness ranged between 6 and 10 mm, where the structure appeared to be equiaxed. On the transverse section, beneath such ring, the structure appeared to radially converge to the metallurgical centre of the billet with well developed dendrites. The metallurgical axis on the longitudinal section which includes the extrados and the intrados of the billet did not coincide with the geometrical axis, and was usually shifted towards the extrados. The maximum observed shift was about 3 mm. On such section the orientation of the dendrites was heading the top of the section, in an angle interval of 7-15 degrees with the transverse direction. "V"-shaped segregation zones are visible, at intervals of roughly 30 millimetres, along the metallurgical axis. The central cavity along the longitudinal section was discontinuous, with metallic bridges connecting the opposite sides of the former solidification fronts, with evidence of sulphur segregation on the bridges, especially just above the cavity (see Figs. 1 and 2).

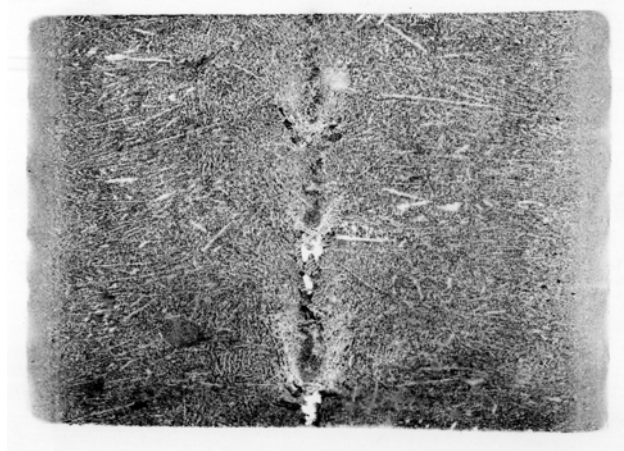


Figure 1. Sulphur print from heat B1. V-shaped segregations are visible as well as the central cavities (white areas) and sulphur-enriched bridges (dark areas)

B. Microstructure

Based on the metallographic etching obtained from the sulphur print technique, quantitative metallography by the linear intercept method was carried out, aimed at the quantification of microstructural parameters such as the primary dendrite arm spacings (PDAS) and secondary dendrite arm spacings (SDAS) in the transverse section of the billets, to allow computations of the local solidification times. Such measurements were carried out also on samples obtained from the usual metallographic preparation route, and etched with the Oberhoffen reagent.

The results obtained by the latter route well fitted with those determined by the former. Of course the values of both the PDAS (λ_1) and the SDAS (λ_2) increased from the zone just beneath the outer ring to the centre of the billets, from values as low as about 200 μm (λ_1) and 55 μm (λ_2), to values as high as 950 μm - 1000 μm (λ_1) and 325 μm - 350 μm (λ_2), respectively.

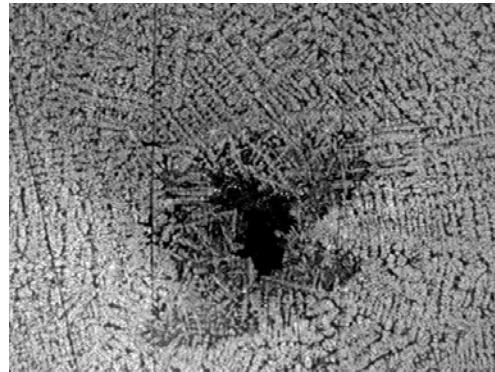


Figure 2. Higher magnification view of the solidification microstructure with evidence of a central cavity

In the annular zone between 57 and 44 mm from the metallurgical centre of the transverse sections of both the heats, a significant slowdown in the rate of λ_1 and λ_2 increase was detected. By computing the local solidification times and according to the casting speed it could be determined that such annular area solidified at a reduced solidification rate, when the billets left the mould and before they reached the primary spray cooling zone.

The overall solidification times, needed for the solidification to develop from the surface of the billet to its center, is determined according to the model proposed by El-Bealy and Thomas [El-Bealy and Thomas, 1996] and assume the values of 465 s and 470 s for heat B1 and B2, respectively.

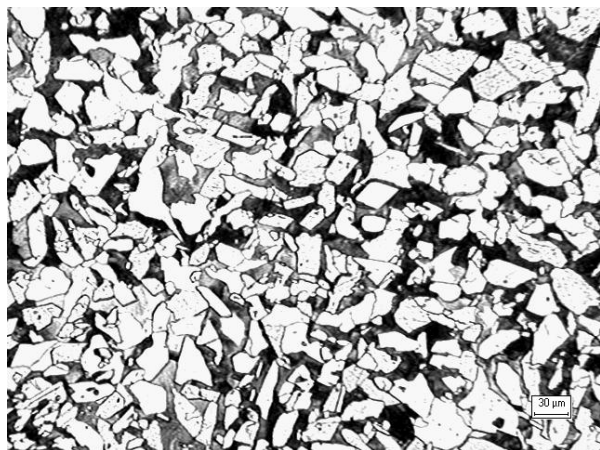


Figure 3. Optical micrograph taken 10 mm beneath the surface on the intrados-extrados diameter (heat B1)

On the basis of metallographic etching using the Nital 3% reagent, an increase in the pearlitic area fraction was determined along the direction from the periphery of the billets towards the metallurgical centre, as shown in Figs. 3 and 4. The pearlite fraction increased from 20% to 25%, which is consistent with the well known increase in carbon content as solidification proceeds towards the metallurgical axis of the billet.

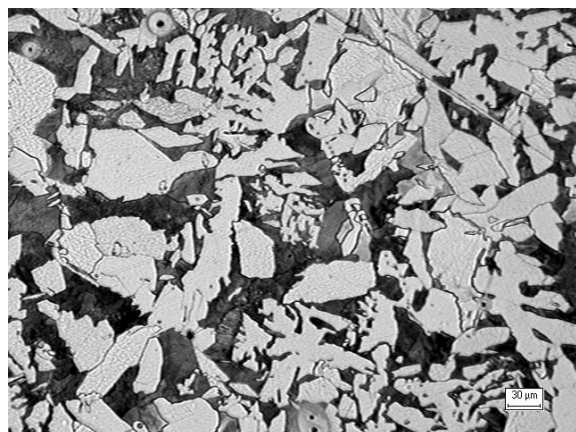


Figure 4. Optical micrograph taken 60 mm from the surface on the intrados-extrados diameter (heat B1)

C. Inclusion distribution

The samples investigated substantially revealed the presence of two different kinds of inclusion types: calcium aluminates and manganese sulphides. Although the presence in small amounts of other elements such as magnesium and titanium was also detected, the inclusion reference system could be reasonably identified with the two above mentioned non-metallic inclusions. The average chemical compositions of the calcium aluminate and of the sulphide inclusions are reported in Tables 2 and 3. From the analyses it can be stated that the calcium aluminates belong to the forms C.2A ($\text{CaO} \cdot 2\text{Al}_2\text{O}_3$) or C.6A ($\text{CaO} \cdot 6\text{Al}_2\text{O}_3$). The presence of the MgO phase is also inferable suggesting the possible

formation of the spinel ($\text{MgO} \cdot \text{Al}_2\text{O}_3$). Considering the low oxygen content of the metal-slag system during alloying by Ca, it is supposed that the MgO oxide was originally contained in the slag or was formed due to metal-refractory lining interaction [Janke 2000].

	Al	Ca	Si	Mn	Mg	S
Average	56	14	3	7	8	12
St dev.	4.8	2.2	2.7	2.8	1.2	2.7

Table 2. Chemical composition (mass %) of the calcium aluminate inclusions detected by EDS microanalysis in the resulphurised steel billets

	Al	Ca	Si	Mn	Mg	S
Average	1	3	2	46	3	45
St dev.	0.9	2.8	1.5	2.3	1.6	2.4

Table 3. Chemical composition (mass %) of the manganese sulphide inclusions detected by EDS microanalysis in the resulphurised steel billets

These values of the compounds are in good agreement with the results of the model describing the inclusions precipitation within the liquid bulk [Mapelli *et al.*, 2000] as calculated by considering the specific chemical compositions of the two steels investigated and the temperature of the liquidus temperature of 1533°C . Table 4 summarises the results obtained by model calculation for the two heats B1 and B2.

Heat	% Al_2O_3	%CaO	%MnS	%CaS
B1	$3 \cdot 10^{-3}$	$4 \cdot 10^{-4}$	$2 \cdot 10^{-2}$	$1 \cdot 10^{-3}$
B2	$3 \cdot 10^{-3}$	$5 \cdot 10^{-4}$	$2 \cdot 10^{-2}$	$2 \cdot 10^{-3}$

Table 4. Computed concentrations (mass %) of the non-metallic compounds formed in the liquid melt at 1533°C

The computations performed pointed out that there is a great presence of MnS, but the amount of CaS is not enough to produce any modifications of MnS. The ratio ($\% \text{Al}_2\text{O}_3 / (\% \text{CaO} + \% \text{Al}_2\text{O}_3)$) is about 0,88 while the experimental value is 0,84.

The experimental chemical compositions gathered in Table 2 were obtained by analysing over 120 non-metallic inclusions. The statistical data demonstrate that there is not a significant variation of the inclusion composition over the examined section of the two billets. Both the C.2A and the C.6A compounds are solid phases during solidification of the steel, their melting temperature being in the range $2048 \div 2176 \text{ K}$ [VDI, 1981]. The presence of solid calcium aluminates during casting is generally considered to be harmful since they can produce nozzle clogging.

For image analysis, the observed non-metallic inclusions were approximated by an equivalent ellipse that contains the inclusion. The calcium aluminate compounds generally featured a round shape with a ratio

between the major and minimum axis close to unity, as shown in figure 5. On the other hand, the manganese sulphides found in the billet structure generally showed a ratio greater than 2 due to their elongated shape, as shown in figure 6. As a first consideration, it is possible to suppose that these non-metallic inclusions belong to the second type of MnS, which feature an elongated shape as a consequence of the oxygen content of the melt that influences the shape and the mechanical properties of the MnS inclusions [Gonzales, 1984]. However, this is not consistent with the calcium-aluminate types found in the billets (C.2A, C.6A) for which $a_{\text{Al}_2\text{O}_3} = 1$, as stated by [Korousic, 1991]. At the casting temperature here used and considering the equilibrium constant: $\log K_{\text{Al}_2\text{O}_3} = 62780/T - 20,17$, the oxygen activity cannot be so high to allow the formation of second type MnS. The above assessment therefore suggests that the shape of MnS is mainly due to their process of formation during the solidification and the related segregation of Mn and S within the dendrite arms.

The average composition of the MnS phase is reported in Table 3. It was obtained by the analysis of over 380 inclusions. During microprobe analyses it was chosen to ignore the presence of the measured Fe on inclusion composition since its contribution was supposed to be mainly due to the steel matrix surrounding the small inclusions. Again, the standard deviation suggests a fairly good homogeneity amongst the sulphides population in both the heats investigated. Traces of Ca and Ti, were also found in the manganese sulphides but it is believed that they cannot cause any important modification to the behaviour and the shape of the inclusions.

The peculiar shape of each inclusion type allowed to distinguish the population of the non-metallic compounds on the basis of their geometrical features during image analysis investigation. This approach may potentially have some drawbacks because some sulphides could have a globular form. However this case was very rare and the measurements were judged sufficiently reliable.

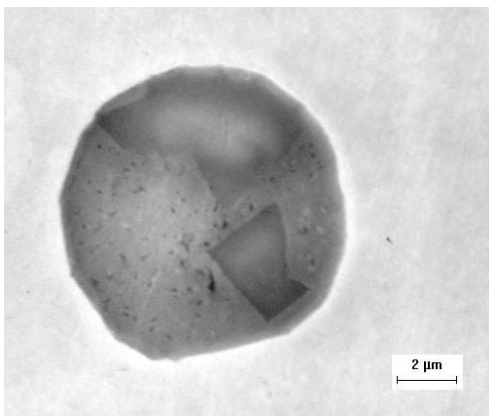


Figure 5. Typical globular calcium aluminate inclusion found in the resulphurised steel

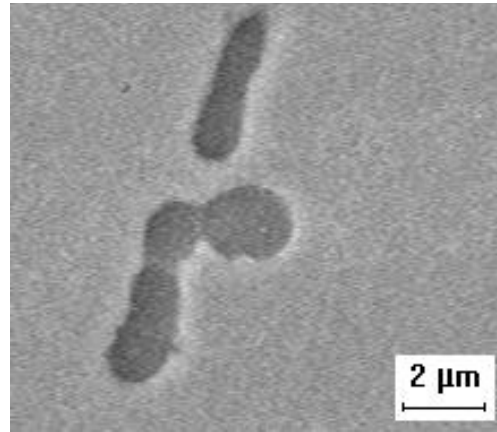


Figure 6. Elongated manganese sulphides found in the resulphurised steel

The total volume fraction of the manganese sulphides and calcium aluminates for the two heats investigated were thus calculated and are reported in Figs. 7 and 8. These data indicate an increase of the volume fraction of the non-metallic inclusions in particular regions, at 20-30mm from the side of the billet.

Further information on the inclusion distribution in the section of the billets are given in the graphs of Figs. 9 and 10, that point out an increase of the manganese sulphide inclusions. A series of peaks positioned at 20-30 mm from the side of the billet is clearly visible; this region roughly corresponds to the area of reduced solidification rate when the billet leaves the mould (previously defined at 57±44 mm from the metallurgical centre).

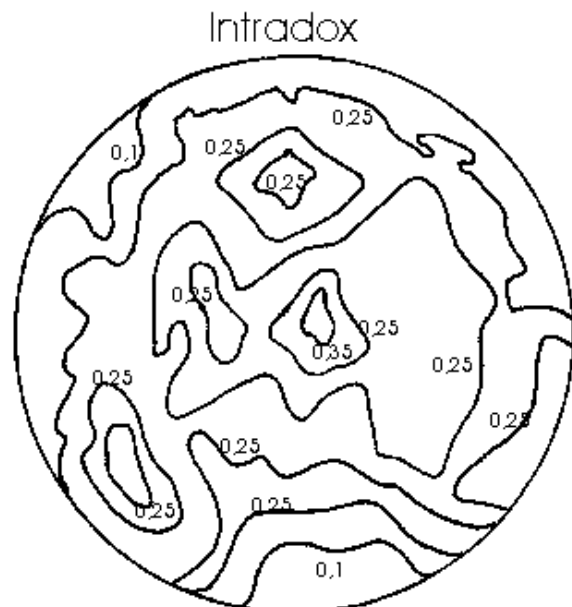


Figure 7. Percentual volume fraction of non-metallic inclusions in billet B1



Figure 8. Percentual volume fraction of non-metallic inclusions in billet B2

Other secondary peaks are distributed in the inner regions featuring irregular spatial distribution presumably due to fluidodynamic effects of the liquid steel flow as affected by nozzle ports inclination, mould geometry and the possible modification of the designed metal flow as a consequence of the deposition of the non-metallic material on the wall of the nozzle (i.e.: possible precipitation of solid calcium aluminates) [Grimm *et al.*, 1999]. Further phenomena of possible influence can be those involving central segregation and floating effects acting together with segregation during the progress of the billet on the curved strand [Bannenberg, 1995].

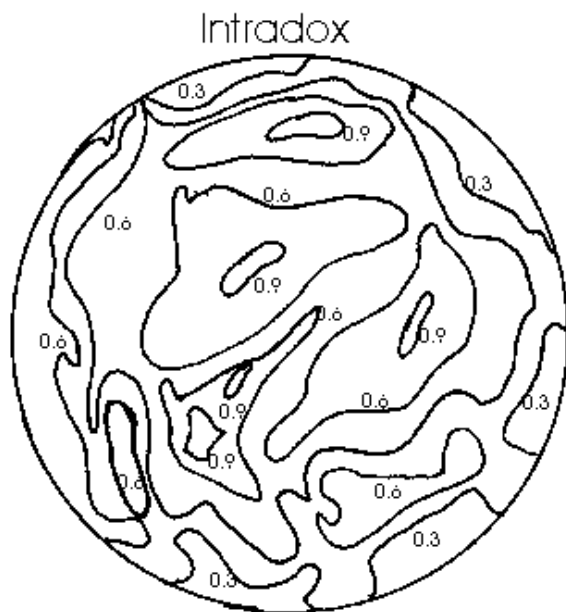


Figure 9 Fraction of MnS on the overall inclusional population detected by image analysis in billets B1

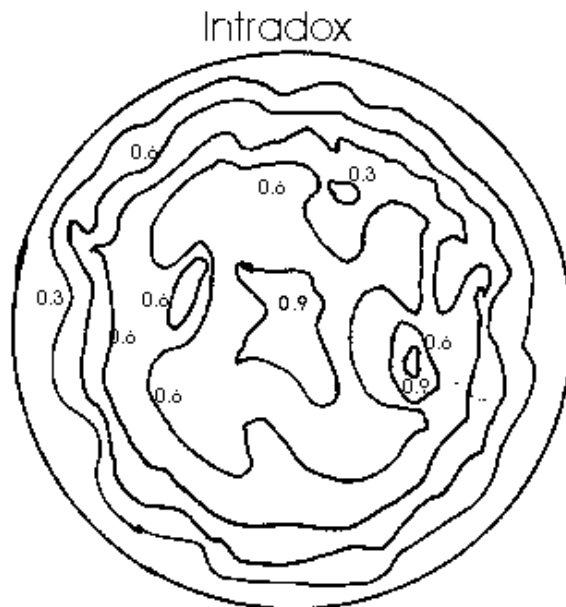


Figure 10 Fraction of MnS on the overall inclusional population detected by image analysis in billets B2

The segregation crown at a distance of 20-30 mm from the outer side is probably determined by a change in the cooling rate that causes the permanence of this region in the range between the solidus and liquidus temperature for a longer time than the other regions. Although such amount of segregation does not lead to any practical concern in the steel products, it has a certain interest for a fundamental study on solidification of resulphurised steels. The features of the development of dendritism in this zone strongly reduces the dilution effects of the solute that segregates between the dendrite arms causing a significant precipitation of the observed non-metallic compounds.

IV. CONCLUSIONS

A study on structure and inclusion distribution as affected by solidification during continuous casting was undertaken on a continuously cast C-Mn resulphurised steel. From experimental analyses carried out on two heats, the following conclusions can be drawn.

- Measurement of primary and secondary dendrite arm spacing allowed to estimate the overall solidification time of the billets as about 470 s.
- An annular zone between 57 and 44 mm from the metallurgical centre of the billets featured a significant slowdown in DAS increasing rate when moving toward billet centre. This was accounted for by a reduction in solidification rate when the billets left the mould and before they reached the primary spray cooling zone.
- Inclusion analysis showed the main presence of manganese sulphides and of calcium aluminates of

the type $\text{CaO} \cdot 2\text{Al}_2\text{O}_3$ and $\text{CaO} \cdot 6\text{Al}_2\text{O}_3$. Detailed image analysis allowed to draw maps of inclusion distribution in the billet section.

- Sulphide segregation regions were detected at positions roughly corresponding to the annular zone of reduced solidification rate. Further inclusion density peaks were measured in the inner zone of the billet sections; these were supposed to be mainly related to irregular fluidodynamic effects of the liquid steel flow.

ACKNOWLEDGEMENTS

The present research was financed by the Italian Ministry of University and Scientific and Technological Research. The authors are also grateful to Dr. Eng. Giovanni Amoruso for his activity in microstructural examinations.

REFERENCES

- Bannenberg, N. *Revue de Metallurgie*, **1**, 63-73 (1995)
- Cicuti, C.E., J. Madias, J.C. Gonzales. *Ironmaking and Steelmaking*, **24**, 2, 155-159 (1997)
- Dyson, D.J., A.J. Rose, M.M. Whitwood, D.P. Wilcox. *Ironmaking and Steelmaking*, **25**, 4, 279-286 (1998)
- El-Bealy, M., H. Fredriksson. *Scandinavian Journal of Metallurgy*, **23**, 140-150 (1994)
- El-Bealy, M., B.G. Thomas. *Metallurgical and Materials Transactions*, **27 B**, 689-692 (1996)
- Eriksson, G., K. Hack. *Metallurgical Transactions*, **21B**, 12, 1013-1023 (1990)
- Gonzales, J.C. *Metalurgia Moderna*, **2**, 1, 29-46 (1984)
- Grimm, B., Andrzejewski, P., Müller, K., Take, K.-H. *Steel Research*, **70**, 10, 420-426, (1999)
- Hassall, G.J., K.G. Bain, R.W. Young, M.S. Millman. *Ironmaking and Steelmaking*, **25**, 4, 273-278 (1998)
- Hong, Z., X. Wu, C. Kun. *Steel Research*, **66**, 2, 72-76 (1995)
- Irving, W.R., A. Perkins, M.G. Brooks. *Ironmaking and Steelmaking*, **11**, 3 152-162 (1984)
- Jacobi, H., K. Wünnenberg. *Steel Research*, **68**, 6, 158-265 (1997)
- Janke, D., Z. Ma, P. Valentin, A. Heinen. *ISIJ International*, **40**, 1, 31-39 (2000)
- Korousic, B. *Steel Research*, **62**, 7, 285-288 (1991)
- Lehmann, J., F. Bertrand, H. Gaye. *La Revue de Metallurgie*, **9**, 1131-1139 (1998)
- Lu, D.-Z., G.A. Irons, W.-K. Lu. *Ironmaking and Steelmaking*, **21**, 5, 362-371 (1994)
- Mapelli, C., W. Nicodemi, M. Vedani, A. Zoppi. *Steel Research*, **71**, 5, 161-168 (2000)
- Presern, V., B. Korousic, J.W. Hastie. *Steel Research*, **62**, 7, 289-295 (1991)
- Senk, D., B. Engl, O. Siemon, G. Stebner. *Steel Research*, **70**, 8/9, 368-372 (1999)

Sivesson, P., G. Hällén, B. Widell. *Ironmaking and Steelmaking*, **25**, 3, 239-246 (1998)

VDI, Schlackenatlas, Düsseldorf, Verlag Stahleisen (1981)

Weisgerber, B., M. Hecht, K. Harste. *Steel Research*, **70**, 10, 403-411 (1999)

Received December 15, 2000.

Accepted for publication, January 15, 2002.

Recommended by Subject Editor E. Dvorkin.